

Conformational Aspects of Poly(*N*-vinylcarbazole)<sup>‡</sup>

P. R. Sundararajan

*Xerox Research Centre of Canada, 2480 Dunwin Drive, Mississauga, Ontario L5L 1J9, Canada. Received December 3, 1979*

**ABSTRACT:** Conformational maps in terms of skeletal bond rotations  $\phi_i$  and  $\phi_{i+1}$  have been calculated for the meso and racemic dyads of poly(*N*-vinylcarbazole) (PVK). The  $\bar{g}$  conformations are ruled out as in the case of other vinyl chains with planar side groups. The energy corresponding to the statistical weight parameter  $\omega''$ , which applies to the *tt* state of the meso dyad, is lower than that for polystyrene, and hence a higher population of the *tt* state can be expected in solution. The contribution of the increase in the *tt* population to the large characteristic ratio of PVK is examined. The calculations also show that a systematic pattern is followed in the shift of the energy minimum from perfect staggering of the bonds in the various states of the meso and racemic dyads. In addition, the chain conformations proposed by Crystal and Griffiths for the crystalline state have been examined, and a conformation with three units in a repeat distance of 6.47 Å is found to be stereochemically favorable.

The importance of poly(*N*-vinylcarbazole) (PVK) as a photoconductive polymer has prompted several studies on its crystalline structure, electrical properties, solution conformations, and characterization by NMR methods. A comprehensive review of the properties of PVK has been given recently by Penwell et al.<sup>1</sup> The crystal structure of PVK was first studied by Kimura et al.,<sup>2</sup> who proposed a stereoblock structure consisting of isotactic threefold helices and syndiotactic twofold helices packed in a hexagonal array. Using electron diffraction patterns from single crystals of PVK, Crystal<sup>3</sup> confirmed the hexagonal symmetry and concluded that the conformation of the polymer was a threefold helix, with a repeat of 7.44 Å. However, from X-ray diffraction studies and density measurements, Griffiths<sup>4</sup> showed that the repeat distance should be about 6.47 Å, similar to that of the Natta-Corradini threefold helical structure for isotactic polystyrene. Recently, it has been shown that the unit cell of PVK is orthorhombic, with pseudohexagonal packing of the chains,<sup>5</sup> with the use of X-ray and electron diffraction patterns from melt-extruded PVK.

Studies on the solution properties of PVK, by Kuwahara et al.<sup>6</sup> and Sitaramaiah and Jacobs,<sup>7</sup> led to the conclusion that the unperturbed dimension of the polymer is rather large and that the steric factor is higher than that for other vinyl chains such as polystyrene. A severe hindrance to free rotation is thus indicated. NMR studies on PVK to determine the tacticity have been unsuccessful, although the spectra recorded by Williams<sup>8</sup> at several temperatures showed that there is hindered rotation within the polymer segments, with an unequal population of conformers.

The conformational analysis of PVK, in terms of pairwise rotations around the skeletal bonds, is presented here. The earlier studies on the conformations of vinyl chains bearing planar substituents, such as poly(methyl methacrylate)<sup>9,10</sup> (PMMA), poly( $\alpha$ -methylstyrene)<sup>11</sup> (PMS), polystyrene<sup>12</sup> (PS), poly(methyl acrylate)<sup>13</sup> (PMA), and poly(vinyl acetate)<sup>14</sup> (PVAc), showed that the planarity of the side group imposes severe restrictions on the available conformations for the pair of bonds comprising the dyad. The  $\bar{g}$  conformations are excluded as a consequence of the planarity of the side group (except in the case of PVAc). The *tt* state of the meso dyad, although of high energy for perfect staggering of the bonds, becomes accessible by a slight synchronized rotation of about 20° from the perfectly staggered conformation. Thus, copious inclusion of *tt* conformations with the *tg* or *gt* state can be expected in

Table I  
Geometrical Parameters

atoms in bond	bond length, Å	atoms in bond	bond angle, deg
C-C	1.53	C-C <sup>α</sup> -C	112
C <sup>α</sup> -H	1.1	C <sup>α</sup> -C-C <sup>α</sup>	variable
		C <sup>α</sup> -N-C <sup>β</sup>	126
		C <sup>β</sup> -N-C <sup>β'</sup>	108
C <sup>α</sup> -N	1.49	N-C <sup>β</sup> -C <sup>γ</sup>	132
C <sup>ar</sup> -N	1.39	C <sup>ar</sup> -C <sup>ar</sup> -C <sup>ar</sup>	120
		C <sup>β</sup> -C <sup>η</sup> -C <sup>η'</sup>	108
C <sup>ar</sup> -C <sup>ar</sup>	1.39	C <sup>η</sup> -C <sup>η</sup> -C <sup>β'</sup>	108

solution. Extended conformations, with the skeletal bonds being close to the *tt*, have been detected in the crystalline gels of isotactic polystyrene<sup>15</sup> and in the crystalline structure of PMMA,<sup>16</sup> both of which bear planar substituents. In comparison to these chains, the side group in PVK is large. The similarity is that it is also planar.

## Conformational Energies

**Parameters for the Calculations.** A segment of an isotactic PVK chain, in the all-trans conformation, is shown in Figure 1, along with the designation of rotations around the bonds. The rotations  $\phi_i$  and  $\phi_{i+1}$  are zero for the trans conformation shown in Figure 1. Following the convention of Flory et al.,<sup>17</sup> viewing always from the C<sup>α</sup> atom to the methylene carbon, rotations about the bond *i* are performed in the right handed sense and those about the bond *i* + 1 are left handed in the case of a meso dyad. The rotations  $\phi_i$  and  $\phi_{i+1}$  are both right handed for the bonds in the racemic dyad. The bond lengths and bond angles used here are given in Table I. The parameters corresponding to the carbazyl group were adapted from crystal structure reports on indole derivatives.<sup>18</sup>

Previous studies on polyisobutylene,<sup>19</sup> PMMA,<sup>9</sup> and PMS<sup>11</sup> showed that due to the size of the side group, the skeletal bond angle  $\theta''$  at the methylene carbon atom<sup>20</sup> is large (122–125°), while the angle at the C<sup>α</sup> atom remains close to 110°. While it is possible that such large values of  $\theta''$  apply to all the conformations of a disubstituted chain, it may be valid only for the *tt* state in a monosubstituted vinyl chain, e.g., PVK. In the other conformations such as *tg* or *gt*, the bond angle  $\theta''$  can be expected to be smaller. Hence, in the present study, the energy maps were computed by letting the bond angle vary from 110 to 126°, in steps of 4° at each ( $\phi_i, \phi_{i+1}$ ) grid point. The carbazyl group was positioned such that the N-C<sup>β'</sup> bond eclipses the C<sup>α</sup>-H bond, which defines  $\chi = 0$ . Due to the bulkiness

<sup>‡</sup> Dedicated to Professor P. J. Flory, on the occasion of his 70th birthday.

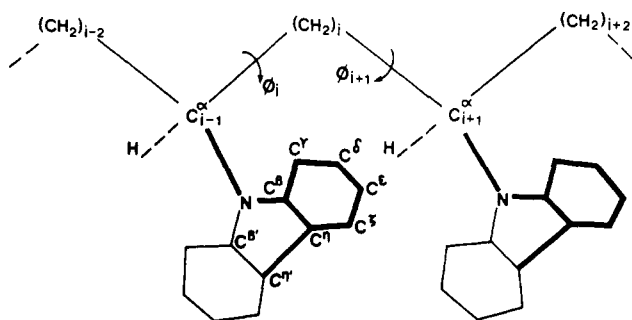


**Figure 1.** A segment of an isotactic PVK chain is shown in the all-trans conformation of the skeletal bonds.

of the side group, the variation in  $\chi$  is expected to be small and hence, as in the calculation for polystyrene,<sup>12</sup>  $\chi = 0$  is used here.

The energies were calculated with the use of the Lennard-Jones 6-12 potential functions for estimating the nonbonded interactions with the same parameters as those used for other vinyl chains.<sup>9-14</sup> Values of 6, 1.15 Å<sup>3</sup>, and 1.45 Å were used for the effective number of electrons, polarizability, and van der Waals radius of the nitrogen atom. A threefold intrinsic torsional potential, with a barrier of 2.8 kcal/mol<sup>-1</sup>, was assigned for the rotations  $\phi_i$  and  $\phi_{i+1}$ . The energy due to the deformation of the skeletal bond angle at the methylene carbon was calculated as before.<sup>9</sup>

A truncation procedure, devised by Yoon et al.<sup>12</sup> and used in the previous calculations on vinyl polymers with planar substituents,<sup>10-14</sup> was followed to allow for the conformational dependence of solvent interactions. In vinyl chains bearing large substituents, the proximity of the side groups, in the *tt* conformation of the meso dyad for example, prevents the access of solvent molecules. In the *gt* or *tg* conformation, however, the interaction between the adjacent side groups is negligible. But this decrease in interaction is compensated for by the interaction between the side group and the solvent molecules, since the former is in a suitable disposition to interact with the solvent. Beyond a certain distance which is sufficient to permit the entry of the solvent molecules, the reduced R...R interaction will be replaced by R...solvent interaction, and the energy of the system should level off at this distance. Thus, the calculated energy remains constant at the value for  $r = \sigma$ , for all distances greater than a suitably chosen value of  $\sigma$ . Values ranging from 3.5 to 5.0 Å have been examined in previous studies.<sup>10-14</sup> Choice of  $\sigma$  depending on the pair of interacting atoms, with  $\sigma = r_i + r_j + 0.2$  (where  $r_i$  and  $r_j$  are the van der Waals radii of the atoms  $i$  and  $j$  and 0.2 is an arbitrary factor), was found best suited for the calculations on PVAc.<sup>14</sup> Values of  $\sigma$  with 3.5, 5.0 Å, and  $r_i + r_j + 0.2$  have been used in the present calculations.

**Results of Energy Calculations.** Conformational energy maps for the meso and the racemic dyads of PVK, using  $\sigma = 5$  Å, are shown in Figures 2 and 3, respectively. Restricted ranges of  $\phi_i$  and  $\phi_{i+1}$ , in the vicinity of *tt*, *gt*, and *gg* states, are presented in these figures. As expected, the *g* conformation is of very high energy, due to the interactions resulting from the planarity of the carbazyl group. The energies of the minima in Figures 2 and 3 are expressed relative to the energy of the *tt* state of the racemic dyad.

Figure 2 for the meso dyad shows that the minima are shifted from perfect staggering in each state. The splitting of the minima into doublets, which is characteristic of disubstituted vinyl chains,<sup>9,11</sup> is absent here. For the

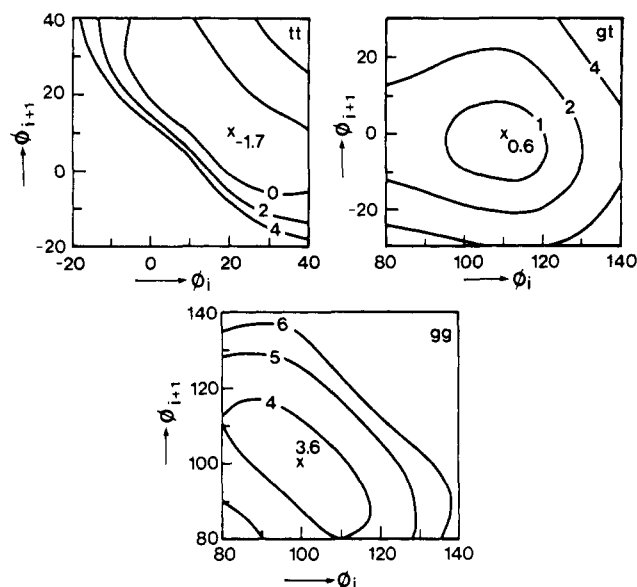


**Figure 2.** Energy contours, in kcal mol<sup>-1</sup>, for the meso dyad are given, in the vicinities of the *tt*, *gt*, and *gg* states. The energies are expressed relative to the minimum for the *tt*, racemic conformation. A value of  $\sigma = 5$  is used.

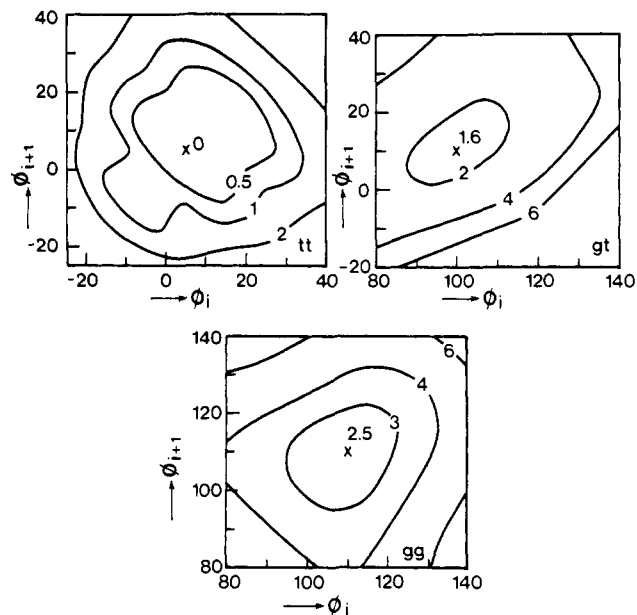


**Figure 3.** Energy contours for the racemic dyad. See legend to Figure 2.

perfectly staggered *tt* state, with  $(\phi_i, \phi_{i+1}) = (0, 0)$ , the energy is very high. The minimum in energy occurs at  $(\phi_i, \phi_{i+1}) = (20^\circ, 10^\circ)$ . The shifts  $\Delta\phi_i$  and  $\Delta\phi_{i+1}$  are both positive (+, +). This is in contrast to the case of disubstituted vinyl chains. For example, in the *tt* state of the meso dyad of PMMA<sup>9</sup>  $\Delta\phi_i$  and  $\Delta\phi_{i+1}$  are of opposite signs, and the minima occur at  $(15, -15)$  and  $(-15, 15)$ . With such a displacement in a disubstituted chain, the interactions  $R_{i-1} \cdots R_{i+1}$  and  $R'_{i-1} \cdots R'_{i+1}$  are simultaneously relieved. The (+, +) shift in the case of PVK is similar to the behavior of monosubstituted chains such as PVAc, PS, and PMA. In this case, the (+, +) shift increases the distance between  $R_{i-1}$  and  $R_{i+1}$ , simultaneously decreasing the  $H_{i-1} \cdots H_{i+1}$  distance slightly. Based on these calculations, it would seem that the generalization made earlier<sup>14</sup> regarding the shifts in energy minima for mono- and disubstituted vinyl chains is valid. This aspect has been discussed in an earlier paper on PVAc<sup>14</sup> and will be discussed further.

The minimum for the *gt* state occurs at (110°, 0°). The energy of this conformation is about 2.3 kcal mol<sup>-1</sup> higher than that at the *tt* minimum. Such a large difference in energy, in favor of the *tt* conformation, is a consequence of the contribution of small attractive energies between several pairs of interacting atoms of the side groups in the *tt* state. This difference in energy depends on the choice of  $\sigma$ , as will be discussed later. The shapes of the energy contours, however, are unaffected by the particular value of  $\sigma$  employed.

The *gg* minimum occurs at (100°, 100°), and the energy of this conformation is large. The (-, -) shift noted in this case is similar to the (+, +) shift for the *tt* state. It increases the distance between the interacting pair (CH<sub>2</sub>)<sub>i-2</sub>... (CH<sub>2</sub>)<sub>i+2</sub> and slightly decreases the distance between H<sub>i-1</sub> and H<sub>i+1</sub>.

Figure 3 shows that the minimum energy for the *tt* state occurs at (5°, 5°) and that of the *gt* state occurs at (100°, 10°). The energy of the *gt* state is about 1.6 kcal mol<sup>-1</sup> higher than that of the *tt* state. The displacements in  $\phi_i$  and  $\phi_{i+1}$  from perfect staggering of the minimum in the *gt* state to (100°, 10°) are of opposite sign, (-, +). Although at first sight it appears to differ from the (+, +) or (-, -) rule stated for the meso dyad, the consequence of the displacement is the same. The (+, +) or (-, -) displacement applies for the meso dyad, in which, according to the convention of Flory et al.,<sup>17</sup> the bonds *i* and *i* + 1 belong to the *d* and *l* species, respectively. The rotations about them are of opposite sense. In the case of the racemic dyad, in which both *i* and *i* + 1 are *d*, the rotation about the bond *i* + 1 is also right handed. Hence, the (-, -) shift in the meso dyad and the (-, +) displacement in the racemic dyad are equivalent.

The *gg* state is about 2.5 kcal mol<sup>-1</sup> higher in energy than the *tt* minimum and occurs at (110°, 110°). The (-, -) shift from perfect staggering increases the distance between interacting pairs (CH<sub>2</sub>)<sub>i-2</sub>...H<sub>i+1</sub> and H<sub>i-1</sub>... (CH<sub>2</sub>)<sub>i+2</sub>, as well as significantly increasing the distance between the diagonally interacting<sup>21</sup> groups (CH<sub>2</sub>)<sub>i-2</sub> and (CH<sub>2</sub>)<sub>i+2</sub>.

On the basis of these and previous calculations, the rules governing the shift of the minima can be stated as follows: (i) The presence of diagonal interactions involving non-hydrogen atoms or groups results in a (-, +) or (+, -) shift in the meso (*dl*) dyad or a (-, -) or (+, +) shift in the racemic (*dd*) dyad. (ii) In the absence of such a diagonal interaction, a (+, +) or (-, -) shift applies for the meso dyad and a (+, -) or (-, +) shift for the racemic dyad. Because of the differences in the skeletal bond angles at the C $\alpha$  atom and the methylene carbon, the shifts in the conformations of the bonds from perfect staggering may have a significant influence on the calculations of properties which are sensitive to geometrical parameters of the chain.

The allowance made for the variation of the bond angle  $\theta''$  in the present calculations leads to interesting results. The preferred bond angle in the minimum energy position in the *tt* state of the meso and racemic dyads is 118°. It decreases to 114° for conformations close to the right-hand top corner of the diagram and increases to 122° in the lower left corner. However, in the *gt* and *gg* states, the preferred  $\theta''$  near the minimum energy position is 114°, and it increases to 118° or 122° in the conformations away from the minimum position. Thus, in the monosubstituted vinyl chains, the larger value of the bond angle  $\theta''$  applies to the *tt* state in which the bulky side chains interact.

The average energy  $\langle E \rangle$ , the partition function *z*, the average bond angle at the methylene carbon  $\langle \theta'' \rangle$ , and the average rotation angles  $\langle \phi_i, \phi_{i+1} \rangle$  were evaluated for each state *s* with the use of energies calculated at intervals of

5° in  $\phi_i$  and  $\phi_{i+1}$ . These are given by

$$z_s = \sum_{\phi_i} \sum_{\phi_{i+1}} \exp(-E_k/RT) \quad (1)$$

$$\langle E \rangle_s = z_s^{-1} \sum_{\phi_i} \sum_{\phi_{i+1}} E_k \exp(-E_k/RT) \quad (2)$$

$$\langle \phi_j \rangle_s = z_s^{-1} \sum_{\phi_i} \sum_{\phi_{i+1}} \phi_j \exp(-E_k/RT) \quad (3)$$

$$\langle \theta'' \rangle_s = z_s^{-1} \sum_{\phi_i} \sum_{\phi_{i+1}} \theta'' \exp(-E_k/RT) \quad (4)$$

where the subscript *k* refers to each conformation ( $\phi_i, \phi_{i+1}$ ) and *j* = *i* or *i* + 1. The results show that the values of  $\langle \phi_i, \phi_{i+1} \rangle$  and  $\langle \theta'' \rangle$  are about the same, irrespective of the value of  $\sigma$  used, although the values of *z* and  $\langle E \rangle$  differ. The preference for the *tt* state of the meso dyad is overwhelming with  $\sigma = 5$ . However, this is drastically reduced with  $\sigma = 3.5$  or  $r_i + r_j + 0.2$ . The results obtained with the latter two values of  $\sigma$  are remarkably similar.

### Statistical Weights

The energies calculated in terms of rotations  $\phi_i$  and  $\phi_{i+1}$  about the bonds *i* and *i* + 1 include the first-order as well as the second-order interactions.<sup>12</sup> The statistical weight matrices for the bond pair *i* and *i* + 1 should therefore include the parameters for both the first- and second-order interactions. With the exclusion of the  $\bar{g}$  state, the matrices reduce to 2 × 2 in order. After normalization with respect to the racemic *tt* state, the matrices  $U_m''$  for the bond pair *i* and *i* + 1 in the meso dyad and  $U_r''$  for the bond pair in the racemic dyad are given by<sup>12</sup>

$$U_m'' = \begin{bmatrix} \omega'' & 1/\eta \\ 1/\eta & \omega/\eta^2 \end{bmatrix} \quad (5)$$

and

$$U_r'' = \begin{bmatrix} 1 & \omega'/\eta \\ \omega'/\eta & 1/\eta^2 \end{bmatrix} \quad (6)$$

The matrix *U'* for the bond pair *i* - 1 and *i* is given by

$$U' = \begin{bmatrix} 1 & 1 \\ 1 & 0 \end{bmatrix} \quad (7)$$

Thus, there are four parameters,  $\omega''$ ,  $\omega'$ ,  $\omega$ , and  $\eta$ , to be evaluated. The interactions they represent have been given before.<sup>12</sup>

A suitable method for deriving the energy corresponding to each parameter, by combining the elements of each state of the matrices  $U_m''$  and  $U_r''$  and the average energies  $\langle E \rangle_s$ , has been given by Suter and Flory.<sup>22</sup> If any one of the statistical weight parameters is given by  $\xi$ , and  $\langle E \rangle_s$  is the energy of the state *s*, the energy  $E_\xi$  corresponding to the parameter  $\xi$  is given by the solution of the overdetermined set of five linear equations<sup>22</sup>

$$\sum E_\xi - \langle E \rangle_s = 0 \quad (8)$$

The five equations comprise the nonequivalent states of the meso and racemic dyads, with the exclusion of the racemic *tt* state, which has the statistical weight of 1.

The differences in the shape and size of the energy domains between the various states are taken into account by introducing a pre-exponential factor  $\xi_0$ , such that

$$\xi = \xi_0 \exp(-E_\xi/RT) \quad (9)$$

The values of  $\xi_0$  corresponding to the four statistical weight

Table II  
Energies and Pre-exponential Factors for the  
Statistical Weight Parameters

parameter	results for		
	$\sigma = 3.5$	$\sigma = 5$	$\sigma = r_i + r_j + 0.2$
$E_{\omega''}$	1.23	-1.81	1.43
$E_{\omega'}$	0.20	0.49	0.25
$E_{\omega}$	0.97	1.17	1.19
$E_{\eta''}$	-0.09	-1.17	0.02
$\omega_{\omega''}$	0.73	0.39	0.72
$\omega_{\omega'}$	0.80	0.76	0.81
$\omega_{\omega}$	0.99	1.04	0.98
$\eta_{\omega}$	1.06	1.15	1.04

parameters can be deduced from the set of five linear equations<sup>22</sup>

$$\sum \ln \xi_0 - \ln z_s - (\sum E_i/RT) = 0 \quad (10)$$

The values of the parameters thus obtained are given in Table II for the various values of  $\sigma$  used here. It is seen that large variations in  $E_{\omega''}$  and  $E_{\eta}$  are seen between the results with  $\sigma = 5$  and  $\sigma = 3.5$  or  $r_i + r_j + 0.2$ . With the former, the values of  $E_{\omega''}$  and  $E_{\eta}$  are significantly negative. Since the gauche states depend inversely on  $\eta$  (see eq 5), an overwhelming preference for the *tt* state is indicated for the meso dyad. A similar difference in the pre-exponential factor  $\omega_{\omega''}$  is also seen. However, the values of  $E_{\omega}$ ,  $E_{\omega'}$ ,  $\omega_{\omega}$ ,  $\omega_{\omega'}$ , and  $\eta_{\omega}$  do not vary significantly with  $\sigma$ . The results obtained with  $\sigma = 3.5$  and  $r_i + r_j + 0.2$  are similar. In the calculations which follow, the parameters  $\omega$  and  $\omega'$  are defined by

$$\omega = 1.0 \exp(-1100/RT) \quad (11)$$

$$\omega' = 0.8 \exp(-500/RT) \quad (12)$$

where the energies are given in calories per mole. The values of  $E_{\omega''}$  and  $E_{\eta}$  were varied to study their effect on the characteristic ratio of the PVK chain. Values of 0.5 and 1.1 were used for  $\omega_{\omega''}$  and  $\eta_{\omega}$ .

### Characteristic Ratios

The characteristic ratios  $C_n = \langle r^2 \rangle_0 / nl^2$  were calculated following the formalism which includes the average location of each of the states of the bond pairs of the dyad.<sup>12</sup> Accordingly,

$$\langle r^2 \rangle_0 = Z^{-1} \mathcal{G}_0 \left( \prod_{k=1}^{x-1} \mathcal{U}' \mathcal{G}_k \right) \mathcal{G}_x \quad (13)$$

The factors  $Z$  and  $\mathcal{U}'$  and the terminal matrices have been defined before.<sup>12,14</sup> The generator matrices for the meso and racemic dyads are given by

$$\mathcal{G}_m = \begin{bmatrix} \omega''(G'G'')_{tt} & (1/\eta)(G'G'')_{tg} \\ (1/\eta)(G'G'')_{gt} & (\omega/\eta^2)(G'G'')_{gg} \end{bmatrix} \quad (14)$$

and

$$\mathcal{G}_x = \begin{bmatrix} (G'G'')_{tt} & (\omega'/\eta)(G'G'')_{tg} \\ (\omega'/\eta)(G'G'')_{gt} & (1/\eta^2)(G'G'')_{gg} \end{bmatrix} \quad (15)$$

The product  $(G'G'')$  is calculated for each of the states by the use of the average torsion angles  $\langle \phi_i \rangle$  and  $\langle \phi_{i+1} \rangle$  and the average bond angle  $\langle \theta'' \rangle$ . The form of the matrix  $G$  has been given before.<sup>12,17</sup>

Calculations were performed by using an average value of  $117^\circ$  for  $\theta''$  in the *tt* state of meso and racemic dyads and a value of  $114^\circ$  for the other states. The average values of the skeletal rotation angles  $(20^\circ, 20^\circ)$ ,  $(110^\circ, 0^\circ)$ , and  $(100^\circ, 100^\circ)$  were used for the *tt*, *gt*, and *gg* states of the meso dyad, respectively;  $(10^\circ, 10^\circ)$ ,  $(100^\circ, 15^\circ)$ , and

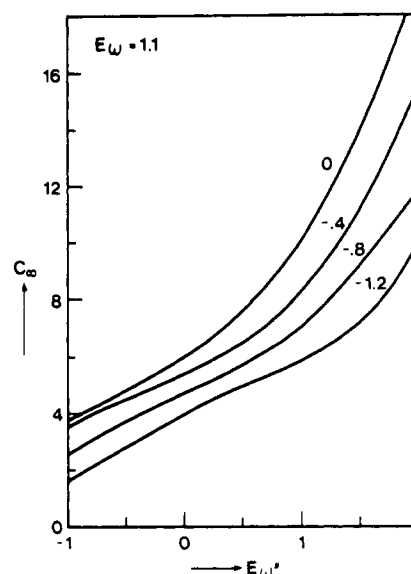
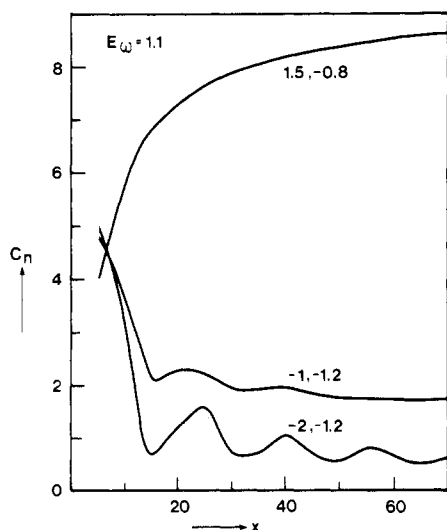


Figure 4. Calculated values of the characteristic ratio for isotactic PVK are given as a function  $E_{\omega''}$  for several values of  $E_{\eta}$  marked on the curves.

$(110^\circ, 110^\circ)$  were used for the same states of the racemic dyad.

The characteristic ratios for an infinite isotactic chain are shown in Figure 4, as a function of  $E_{\omega''}$ , for several values of  $E_{\eta}$ . Irrespective of the value of  $E_{\eta}$ , the value of  $C_\infty$  is small for negative values of  $E_{\omega''}$  and increases sharply between 0 and 2 kcal mol<sup>-1</sup>. An excessive preference for the *tt* state occurs with low values of  $E_{\omega''}$ . Due to the difference of  $5^\circ$  in the skeletal bond angles at the C $^\alpha$  atom and the methylene carbon atom, there is a tendency to form a polygonal shape, leading to small values of  $C_\infty$ . The *gt*, *tg*, and *gg* states depend inversely on  $\eta$ . Thus, when the value of  $E_{\eta}$  increases, an increase in the population of the gauche states disrupts the *tt* perpetuation, leading to an increase in  $C_\infty$ . With an increase in  $E_{\omega''}$ , the occurrence of *tt* and *gt* states is comparable and hence  $C_\infty$  increases drastically. Comparing Figure 4 with Figure 6 of ref 12 for isotactic polystyrene, although the shapes of the curves are similar, the values of  $C_\infty$  for the same values of  $E_{\omega''}$  and  $E_{\eta}$  are higher for PVK than for polystyrene. This is due to the following: (a) the value of  $E_{\omega}$  in the case of PVK being 1100 cal mol<sup>-1</sup> compared to  $\sim 2000$  cal mol<sup>-1</sup> for polystyrene; and (b) a constant value of  $114^\circ$  was used for all the states of polystyrene, whereas a higher value of  $117^\circ$  is used here for the *tt* state alone. Perpetuation of the *tt* state in this situation leads to a small  $C_\infty$ , and inclusion of *tg* and *gg* states increases its value. On the other hand, predominance of the *tg* or *gt* state leads to helical segments, leading to large values of  $C_\infty$ , and the occurrence of the *tt* state in an otherwise helical sequence interrupts the helix propagation and reduces the value of  $C_\infty$ . This statement is supported by the calculations published so far on vinyl chains with unequal skeletal bond angles.

The effect of a small value of  $E_{\omega''}$  is shown in Figure 5, in which the values of  $C_n$  are plotted as a function of  $x$ , the number of units in the chain. It is seen that for low values of  $E_{\omega''}$ , the characteristic ratio decreases up to  $x \approx 15$  and oscillates thereafter until  $x \approx 100$ . However, a monotonic increase of  $C_n$  with  $x$  is found when  $E_{\omega''}$  is large. Even with  $E_{\omega''} = 1.5$  kcal mol<sup>-1</sup>, the asymptotic value of  $C_n$  is not reached until  $x \approx 70$ . The measurements of hypochromism of PVK by Tsuchihashi et al.<sup>23</sup> showed that the intensities of the UV absorption intensities decreased from a molecular weight of 1200 up to about 10 000 after



**Figure 5.** Values of  $C_n$  are plotted, for isotactic PVK, as a function of the number of units in the chain. Values of  $E_{\omega''}$  and  $E_{\eta}$ , in that order, are marked on the curves.

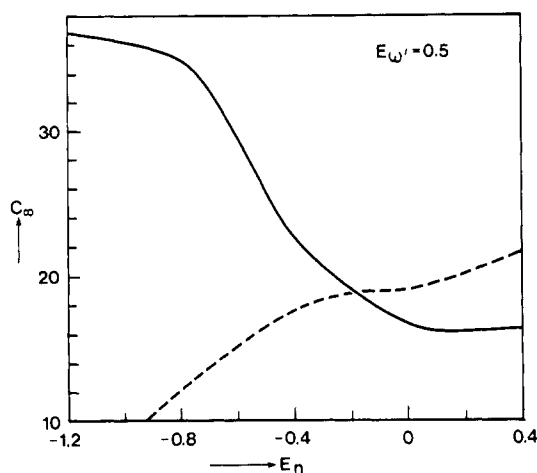


**Figure 6.** The characteristic ratios for a syndiotactic PVK chain are plotted as a function of  $E_{\eta}$ . The dashed curve corresponds to the chain with  $\theta'' = 125^\circ$ .

which they were constant. The molecular weight of 1200 corresponds to about 12 units and the higher molecular weight of 10 000 to about 104 units. According to their results,<sup>23</sup> the rigid local structure of PVK only begins with a molecular weight of 1200.

The characteristic ratio  $C_{\infty}$  for the syndiotactic chain of PVK is shown in Figure 6 as a function of  $E_{\eta}$ . As the value of  $E_{\eta}$  is increased, a drastic reduction in  $C_{\infty}$  is noted in the region from  $-0.8$  to  $0$  kcal mol<sup>-1</sup>. The effect of the bond angle  $\theta''$  is also illustrated in Figure 6. The dashed curve corresponds to a value of  $\theta'' = 125^\circ$ . It is seen that for low values of  $E_{\eta}$ , in which case the *gt* and *gg* populations are suppressed, the  $C_{\infty}$  is small.

Characteristic ratios for stereoirregular chains of PVK are shown in Figure 7, for select values of  $E_{\omega''}$  and  $E_{\eta}$ . Monte-Carlo chains of 200 units each were generated to calculate  $C_n$ , and the average of 20 such chains was taken. It is seen that  $C_n$  increases with  $E_{\eta}$  for the isotactic chain and the curve becomes concave. The large value of  $C_n$  in the range of  $f_i = 0.2$ – $0$ , shown by the dot-dash curve, is primarily due to the value of  $E_{\eta}$ . Experimental results on the unperturbed dimensions of PVK are very few. The values of the characteristic ratio deduced by Sitaramaiah and Jacobs<sup>7</sup> and Kuwahara et al.<sup>6</sup> are 16.9 and 18.2, respectively. The tacticity of the samples used in these

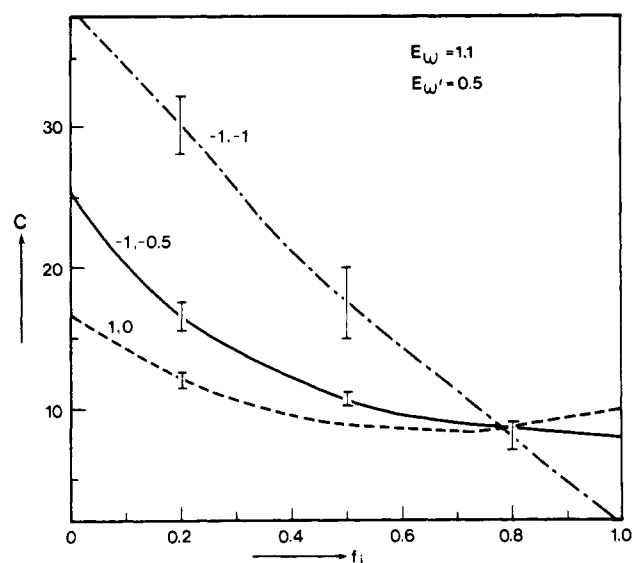


**Figure 7.** The characteristic ratios for Monte-Carlo chains of 200 units are plotted as a function of the isotacticity. Values of  $E_{\omega''}$  and  $E_{\eta}$ , in that order, are marked on the curves. Standard deviations of less than 0.5 are not shown.

experiments is not known. The difficulties associated with the measurements of the tacticity of PVK by NMR methods have been outlined by Williams.<sup>8</sup> However, the experimental values are reproduced by the curves for  $E_{\omega''} = -1$  to  $1.0$  and  $E_{\eta} = -0.5$  or  $0$  kcal mol<sup>-1</sup> for a chain with about 80% syndiotacticity. The values of  $E_{\omega''}$  above  $1.0$  kcal mol<sup>-1</sup> tend to reduce the characteristic ratio for stereoirregular chains with  $f_i > 0.5$ . Thus, the statistical weights  $\omega''$  and  $\eta$  for PVK may be expressed as

$$\omega'' \approx 0.5 \exp(-1000/RT) \quad (16)$$

and

$$\eta \approx 1.1 \exp(500/RT) \quad (17)$$

On the basis of these calculations, the large value of the characteristic ratio of the PVK chains may be interpreted as being due to the lower value of  $E_{\omega''}$  compared to the case of, e.g., polystyrene. Competing contributions due to the *tt* and *gt* states and the unequal values of the skeletal bond angles might play a significant role in giving rise to a large characteristic ratio.

### Helical Conformation in the Crystalline State

It was mentioned before that Crystal<sup>3</sup> proposed a threefold helical conformation with a repeat of  $7.44$  Å for the crystalline state of PVK. Griffiths,<sup>4</sup> however, deduced a smaller repeat of  $6.47$  Å and commented that the larger repeat suggested by Crystal would require a larger skeletal bond angle. In view of the preference for a larger bond angle  $\theta''$  in vinyl chains with bulky substituents, the stereochemical feasibility of both structures is examined here.

In order to compare the two helical structures, the virtual bond method<sup>24</sup> is used here. The application of this method to the crystalline conformations of vinyl chains has been given before.<sup>25</sup> Essentially, with the virtual bond (or the end-to-end vector) of the repeating unit at the proper tilt with respect to the helix axis, as dictated by the helical parameters, a rotation  $\theta$  is applied to the rest of the atoms of the repeat unit in order to vary their disposition with respect to the helix axis. Contiguous units are generated for each  $\theta$ , and the parameters  $\theta''$ ,  $\phi_i$ , and  $\phi_{i+1}$  and the dyad energy can be calculated. This is a simple method for examining the conformations of a helix, with various values of  $\theta''$ .

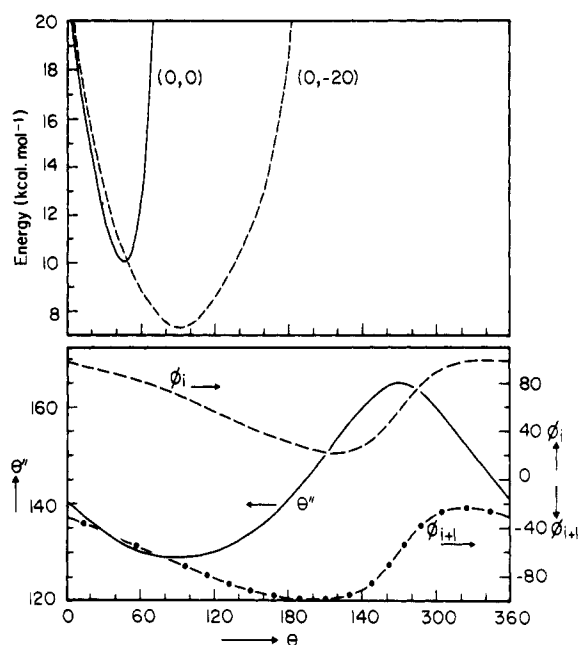


**Figure 8.** Results of the virtual bond analysis for the 3(2.48)-helix are shown. The values of  $\theta''$  (left ordinate) and  $\phi_i$  and  $\phi_{i+1}$  (right ordinate) are plotted as a function of the virtual bond rotation angle  $\theta$ . The energies are given in the upper part of the diagram.

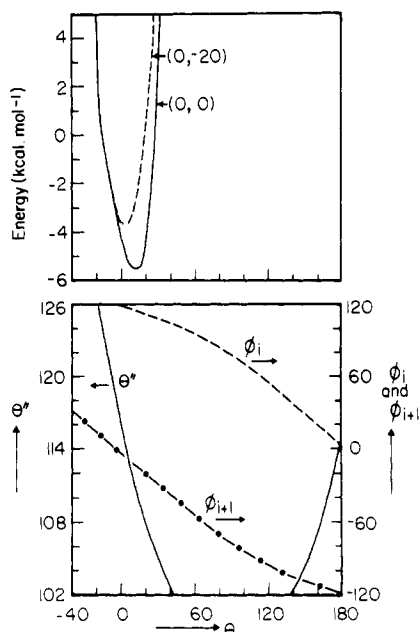


**Figure 9.** Results of the virtual bond analysis for the 3(2.16)-helix are shown. See the legend to Figure 8.

Figure 8 shows the results of such an analysis for the right handed 3(2.48)-helix<sup>26</sup> (with the repeat of 7.44 Å). The calculated values of  $\theta''$ ,  $\phi_i$ , and  $\phi_{i+1}$  are plotted as functions of the virtual bond rotation angle  $\theta$ , in the lower half of the figure. The corresponding dyad energies are given in the upper half for two values of the side group rotations. The energy calculations were performed with the parameters defined before, but the van der Waals radii were reduced by 0.1 Å for the crystalline state. Figure 8 shows that in the entire range of the virtual bond rotation, from 0 to 360°, the bond angle  $\theta''$  varies from 128 to 165°. The minimum in energy with  $(\chi_{i-1}, \chi_{i+1}) = (0,0)$  occurs at  $\theta = 48^\circ$ , with values of  $\theta'' = 132^\circ$ ,  $(\phi_i, \phi_{i+1}) = (88^\circ, -50^\circ)$ ,

and an energy of 10 kcal mol<sup>-1</sup>. With  $(\chi_{i-1}, \chi_{i+1}) = (0, -20^\circ)$ , the energy is reduced to 7.3 kcal mol<sup>-1</sup> and the minimum shifts to  $\theta = 90^\circ$ , with  $\theta'' = 129^\circ$  and  $(\phi_i, \phi_{i+1}) = (70^\circ, -70^\circ)$ . Any other set of side group rotations does not decrease the energy. The values of  $\phi_i$  and  $\phi_{i+1}$  for the 3(2.48)-helix are close to the eclipsed conformation of the skeletal bonds, and the value of  $\theta''$  required to generate this helix is large.

The results corresponding to the 3(2.16)-helix are shown in Figure 9. A restricted range of  $\theta$  is shown here. It is seen that the minimum in energy, with  $(\chi_{i-1}, \chi_{i+1}) = (0,0)$ , occurs at  $\theta = 10^\circ$ , with  $\theta'' = 112^\circ$ , and  $(\phi_i, \phi_{i+1}) = (116^\circ, -10^\circ)$ , with an energy of -5.5 kcal mol<sup>-1</sup>. Varying the side group rotation angles does not decrease the energy in this case. It is interesting that the preferred value of  $\theta''$  is 112°. Such a low value is due to the absence of strong interactions involving the bulky side chain with atoms or groups of the adjacent C $\alpha$  atom.

Comparison of Figures 8 and 9 shows that the energy of the 3(2.16)-helix is significantly lower than that of the 3(2.48)-helix. This is due to the fact that in spite of the allowance for a large value of  $\theta''$ , the 3(2.48) can be constructed only with near-eclipsed conformations of the skeletal bonds, with  $(\phi_i, \phi_{i+1}) = (70^\circ, -70^\circ)$ . Thus, the 3(2.48)-helix is stereochemically unfavorable.

**Acknowledgment.** The author is grateful to Drs. R. H. Marchessault and M. L. Hair of this research center for their interest in this work.

## References and Notes

- (1) R. C. Penwell, B. N. Ganguly, and T. W. Smith, *J. Polym. Sci., Macromol. Rev.*, **13**, 63 (1978).
- (2) A. Kimura, S. Yoshimoto, Y. Akana, H. Hirata, S. Kusabayashi, H. Mikawa, and N. Kasai, *J. Polym. Sci., Part A-2*, **8**, 643 (1970).
- (3) R. G. Crystal, *Macromolecules*, **4**, 379 (1971).
- (4) C. H. Griffiths, *J. Polym. Sci., Polym. Phys. Ed.*, **13**, 1167 (1975); *J. Polym. Sci., Polym. Lett. Ed.*, **16**, 271 (1978).
- (5) P. R. Sundararajan and J. Zamin, *Polymer*, **20**, 1567 (1979).
- (6) N. Kuwahara, S. Higashida, M. Nakata, and M. Kaneko, *J. Polym. Sci., Part A-2*, **7**, 285 (1969).
- (7) G. Sitaramaiah and D. Jacobs, *Polymer*, **11**, 165 (1970).
- (8) D. J. Williams, *Macromolecules*, **3**, 602 (1970).
- (9) P. R. Sundararajan and P. J. Flory, *J. Am. Chem. Soc.*, **96**, 5025 (1974).
- (10) P. R. Sundararajan, *J. Polym. Sci., Polym. Lett. Ed.*, **15**, 699 (1977).
- (11) P. R. Sundararajan, *Macromolecules*, **10**, 623 (1977).
- (12) D. Y. Yoon, P. R. Sundararajan, and P. J. Flory, *Macromolecules*, **8**, 776 (1975).
- (13) D. Y. Yoon, U. W. Suter, P. R. Sundararajan, and P. J. Flory, *Macromolecules*, **8**, 784 (1975).
- (14) P. R. Sundararajan, *Macromolecules*, **11**, 256 (1978).
- (15) E. D. T. Atkins, D. H. Isaac, A. Keller, and K. Miyasaka, *J. Polym. Sci., Polym. Phys. Ed.*, **15**, 211 (1977).
- (16) H. Kusanagi, H. Tadokoro, and Y. Chatani, *Macromolecules*, **9**, 531 (1976).
- (17) P. J. Flory, P. R. Sundararajan, and L. C. DeBolt, *J. Am. Chem. Soc.*, **96**, 5015 (1974).
- (18) B. K. Vijayalakshmi and R. Srinivasan, *Acta Crystallogr., Sect. B*, **31**, 999 (1975), and references therein.
- (19) E. Benedetti, C. Pedone, and G. Allegra, *Macromolecules*, **3**, 16, 727 (1970).
- (20) Note that this bond angle has been denoted by  $(\pi - \theta')$  in the convention of Flory.<sup>9,13</sup>
- (21) The diagonal interactions<sup>9,11</sup> are those between groups attached to C $\alpha_{i-1}$  and C $\alpha_{i+1}$  and which are on opposite sides of the plane defined by the skeletal bonds  $i$  and  $i + 1$ .
- (22) U. W. Suter and P. J. Flory, *Macromolecules*, **8**, 765 (1975).
- (23) N. Tsuchihashi, T. Enomoto, K. Tanikawa, A. Tajiri, and M. Hatano, *Makromol. Chem.*, **176**, 2833 (1975).
- (24) P. R. Sundararajan and R. H. Marchessault, *Can. J. Chem.*, **53**, 3563 (1975).
- (25) P. R. Sundararajan, *Macromolecules*, **12**, 575 (1979).
- (26) In this notation,  $n(\pm h)$  refers to a helix with  $n$  monomers per turn, with an advance per monomer of  $h$  along the helix axis. The negative sign applies to the left-handed helix.